*Available online at* www. scholarsresearchlibrary.com

Scholars Research Library

Der Pharmacia Lettre, 2021, 13(3): 14-20
*(http: //scholarsresearchlibrary. com/archive. html)*

ISSN 0975-5071
USA CODEN: DPLEB4

# Structure and Electronic of the $Ag/BaFe_2As_2$ Interface: A First Principle Study

**Imen Hassaine[1], Abdelouahab Ouahab[2]**

[1]*Laboratories for New and Renewable Energies in Arid Zones (LENREZA), University of Ouargla, Algeria.*

[2]*Department of Material Sciences, University of Biskra, Algeria.*

[*]***Corresponding author:*** *Imen Hassaine, Laboratories for New and Renewable Energies in Arid Zones (LENREZA), University of Ouargla, Ouargla, Algeria, E-mail: hassainebouazza@yahoo.fr*

## ABSTRACT

*The pseudo-potentiel method based on density functional theory (DFT) using the generalized gradient approximation (GGA) is applied to study the structural and electronic properties of the interface $Ag/BaFe_2As_2$ (001) between the iron pnictide superconductor $BaFe_2As_2$ and silver. In this study three configurations of the structure are considered. The variation of interaction energy with respect to the distance separating the two materials endorses the possibility of interface formation. The deposition of silver atoms on the intermediate sites of the superconductor surface averred to be the most stable configuration. The comparison between the obtained total and partial electronic densities of states before and after the formation of the interface shows a slight change in the distribution of electronic states with a shift in the vicinity of the Fermi energy. In this study we consider the interface as metallic, in spite of the coexistence of the covalent-like and metallic bonds as shown by the analyses of the distribution of the electronic charge density.*

**Keywords:** *Iron pnictide superconductor, $BaFe_2As_2$, Metal interface, DFT, Electronic Properties, Interaction Energy*

## INTRODUCTION

The metal-superconductor conventional interfaces have been subjected to a growing research nowadays owing to recent experimental developments in preparation and characterization techniques at the atomic scale under ultrahigh vacuum [1-3]. Systems like metal-superconductor interfaces have been studied theoretically by several methods such as first principles techniques which are used to solve the atomic and electronic structure of complex systems [4-6]. When they are used in electrical circuits, the very intense electric currents flowing through the superconducting metal interface require very good electrical contacts. These systems have various properties that promote their application in many areas of technology such as spintronics, magnetic memories [7], instruments based on superconductors and in high magnetic field instruments such as nuclear magnetic resonance (NMR) equipments [8]. The generation of high intensity magnetic fields requires electric current densities in the range of 104-106 A/m2 [9-11]. Many studies have been carried out on the new iron-pnictide

superconducting compounds such as LaOFeAs and $AFe_2As_2$ (A=K, Ba, Sr, and Cs) as a function of doping or applied pressure [12].

The $BaFe_2As_2$ system, also known as the 122 compound [13], exhibits a superconducting critical temperature at about 55 K [13]. The crystal structure of $BaFe_2As_2$, made by alternating FeAs planes and Ba layers, is tetragonal with the I4/mmm space group. At T ~ 143 K, $BaFe_2As_2$ undergoes a structural phase transition from tetragonal to an orthorhombic phase of the Fmmm space group [14].

This superconductor is considered as a model system in the pnictide family. It is subjected to numerous experimental and theoretical studies [15-17] where the investigation was focused on structural, electronic and magnetic properties. There is also the challenge of discovering the microscopic mechanisms give these systems their superconductor state which is recognized to be different from the conventional superconductors [18]. Despite the numerous studies on the different bulk properties of this superconductor, no studies on metal/$BaFe_2As_2$ interfaces are available to our knowledge. The present study is interested mainly with the structural and electronic properties of the interface between a noble metal (silver) and the $BaFe_2As_2$ surface.

## MATERIALS AND METHODS

Although structural and electronic properties of the tetragonal phase (4 mm) of $BaFe_2As_2$ were investigated both experimentally and theoretically in previous studies, not much is known about their properties when interfaced with other metals. In this study, we have performed DFT calculations using the 'pseudo-potential' method [19] implemented on the Quantum ESPRESSO PWSCF computer code with the generalized gradient approximation (GGA) parameterized by Perdew, Burke and Ernzerhof [20].

In order to calculate the interaction energies between a metallic film and a superconductive substrate, we used the 'ultra-soft' pseudo-potential type. An abrupt interface model between the Ag film and the pnictide superconductor is proposed where the Ag atoms are positioned on top of the Ba termination surface of the superconductor. The optimized structure of the iron based pnictide superconductor $BaFe_2As_2$ was achieved by the relaxation of a tetragonal unit cell containing 10 atoms. The obtained unit cell parameters a, b, and c, were 3.960, 3.960 and 13.010 Å respectively. The equilibrium atomic positions were also determined [21]. For the silver structure, we used the experimental estimated unit cell parameter of 4.09 Å. The Ag film is supposed to be rigid (the atoms occupy their bulk positions) and is represented by 5 atomic monolayers parallel to the (001) surface of an FCC unit cell. These monolayers are distributed symmetrically on the top and the bottom of the $BaFe_2As_2$ surfaces as shown in Figure 1. This structure is adopted to save the mirror symmetry of the substrate. The electronic configuration used for As, Ba, Fe and Ag were 4s24p3, 5s25p65d06s22s22p3, 2p63s13p1, and 3d74s1, respectively. The cut-off energy and the k-points mesh were optimized using the experimental unit cell parameters of the $BaFe_2As_2$ unit cell, ranging from 20 to 100 Ry. it is found that 35 Ry is reasonable and provides a good compromise between accuracy and computation time. The k-points mesh is optimized to a 9 x 9 x 3 sampling of the first Brillouin zone of the reciprocal space corresponding to the supercell of the model. It should be noted that during the minimization of total energy of the studied systems, we imposed a value of 10-6 eV as a convergence energy threshold. The maximum tolerated force on each atom is below 10-3 eV/Å.

To establish the most favorable deposition sites for Ag atoms on the superconductor surface, i.e. barium sites or hollow sites, we have determined the interaction energy between the two materials forming the interface, the Ag film and the substrate, with respect to the separation distance at the interface. The interaction energy can be calculated by the following equation:

$$E_{int}(d) = \frac{1}{2}(E_{tot} - E_{Ag} - E_{sup}) \qquad (1)$$

Where d is the distance separating the superconductor and the metal Figure 1.

Etot, E Ag and E sup in this formula mean the total energies of the supercell, the metal layer with its surface and the substrate with its surface $BaFe_2As_2$ respectively. The factor ½ in this equation is due to the existence of the two interfaces in the supercell.

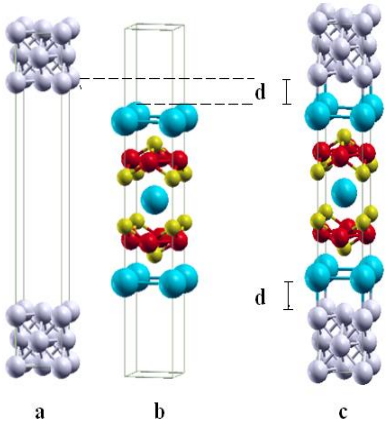


**Figure 1:** Systems used to calculate the interaction energy for each configuration of the interface. **Figure 1A and 1B:** separated metal and superconductor systems**, Figure** C: The super cell representing Ag/$BaFe_2As_2$ (001) interface where d is the vertical distance of separation between the metal and the superconductor.

---

## RESULTS

***Structural optimization of $BaFe_2As_2$***

The structure of $BaFe_2As_2$ with tetragonal symmetry was optimized for the non-magnetic state. The atomic structure was obtained after a relaxation process where all the atomic positions and lattice parameters were optimized. The results are reported in reference [21]. We used these results to construct the interface between Ag and a $BaFe_2As_2$ substrate which we considered to be rigid as shown in Figure1A.

***Ag/$BaFe_2As_2$ interface***

The results of the atomic structure of the Ag/$BaFe_2As_2$ (001) interface at the atomic scale are presented. Three of high symmetry configurations as illustrated in Figure 2 will be used to determine the interaction between the silver film and $BaFe_2As_2$. The first configuration of the interface is related to the state in which surface Ag atoms are on top of Ba atoms of the (001) surface while the second one concerns the Ag atoms in the middle of the rib connecting two atoms of barium Ba-Ba. The third configuration deals with an intermediate state between configurations 1 and 2. Refer to states (I), (II) and (III) of Figure 2 respectively.

The variation of the interface interaction energy for these three configurations with respect to the distance between the two materials Ag and $BaFe_2As_2$ is displayed in a Morse- type potential is used to fit the effective interactions between atoms of both sides of the abrupt interface. The analytical form of our Morse potential is given by:

$$E_{int}(d) = A_0[(e^{-2A_1(d-A_2)} - 2e^{-A_1(d-A_2)}] \quad (2)$$

Where $A_0$ and $A_2$ are the constants used to determine the energy and distance of separation at minimum energy. The fitting shows that the intermediate state is the most favorable with a separation distance d = 2.944 Å and an interaction energy of -0.0835 Ry, while the results of separation distance and interaction energy for the first and the third configurations are (3.143 Å, 3.015 Å) and (-0.0683Ry, -0.0795Ry) respectively.

The variation of the interface interaction energy for these three configurations with respect to the distance between the two materials Ag and $BaFe_2As_2$ is displayed. A Morse- type potential is used to fit the effective interactions between atoms of both sides of the abrupt interface.

The analytical form of our Morse potential is given by:

$$E_{int}(d) = A_0[(e^{-2A_1(d-A_2)} - 2e^{-A_1(d-A_2)}] \quad (2)$$

Where $A_0$ and $A_2$ are the constants used to determine the energy and distance of separation at minimum energy. The fitting shows that the intermediate state is the most favorable with a separation distance d = 2.944 Å and an interaction energy of -0.0835 Ry, while the results of separation distance and interaction energy for the first and the third configurations are (3.143 Å, 3.015 Å) and (-0.0683Ry, -0.0795Ry) respectively.

The results of the atomic structure of the Ag/$BaFe_2As_2$ (001) interface at the atomic scale are presented. Three of high symmetry configurations as illustrated in Figure 2 will be used to determine the interaction between the silver film and $BaFe_2As_2$. The first configuration of the interface is related to the state in which surface Ag atoms are on top of Ba atoms of the (001) surface while the second one concerns the Ag atoms in the middle of the rib connecting two atoms of barium Ba-Ba.

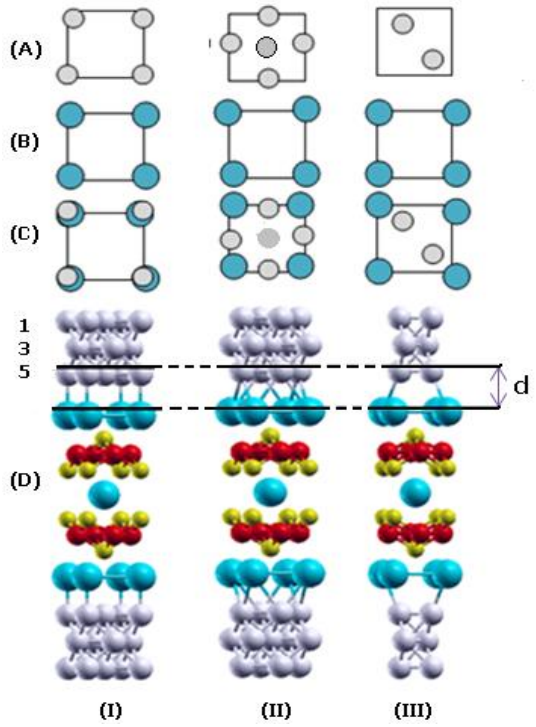


**Figure 2:** Structure of Ag and $BaFe_2As_2$ (001) surfaces, (2): the three configurations of high symmetries: (I) silver atoms are on top of barium sites, (II) Ag atoms are on the middle of the rib connecting the two atoms of barium, and (III) configuration concerns an intermediate situation between configuration (I) and (II).1, 3 and 5 are the numbers of atoms in the structure of silver.

### *Charge density*

The charge density is calculated and presented in the form of contours for the three interface configurations. Focusing our study on the surface containing the barium and silver atoms, the results obtained for the three configurations (I),(II) and (III) are shown respectively.

However, this plane does not give enough information about barium and silver atoms in configurations (III) that is why we have added another plane. We note that in all cases the valence electronic charge for the Ba-Ba bond is concentrated around barium atomic positions in the three configurations, while it is very minimal in the region between the atoms (0.0063, 0.0073 and 0.0066) electrons/Å3 .On the other hand, the Ba-Ag bond is polarized closer to the more electronegative silver atoms (0.4076, 0.4025 and 0.4046) electrons/Å3.

The high concentration of electrons in the regions between the nearest neighbor atomic sites represents the polar covalent bonds between these atoms. With regard to the electronic distribution in Ag-Ag bonds, the electron density around silver atoms varies around the values 0.4025, 0.0301 and 0.4076 electrons/Å3 for the three monolayers respectively. The same fact is observed for the bonds between iron atoms which are is characterized by a high charge density around Fe ions which is due to Fe-3d orbitals. Each Fe atom forms three bonds with arsenic atoms (As–Fe–As) in tetrahedral directions.

To sum up we can infer that the results of charge density concerning the Ba-Ba and Fe-As bonds are in good agreement with our study of charge density for the $BaFe_2As_2$ substrate compounds. The presence of metallic and polar-covalent bonds leads to the most stable third configuration, characterized by the lowest interaction energy

## DISCUSSION

In this section, we compare the total density of states (DOS) and partial density of states (PDOS) for the original $BaFe_2As_2$ compound and $Ag/BaFe_2As_2$ (001) interface for the three configurations (I), (II) and (III).

We note that the contribution of iron in the three configurations is very similar to the original compound [21, 22], especially the Fe-3d orbital, opposing to the contribution of Ba-6p, which is slightly increased in the energy range between -3 and 3 eV. The same facts are observed for the As-4p orbital which is characterized by an increase of density of states at -3.3 eV and -4.6 eV peaks. We also note that there is no change in the PDOS for all $BaFe_2As_2$ atoms in the vicinity of the Fermi energy.

A slight shift of the iron 3d peak is observed for the configurations (I) and (II) in the interface with respect to the bulk while it is identical to its shape within the bulk for the third configuration. The iron atoms prefer not to be involved in the formation of the interface. For the silver atoms, the most contributing orbital is 4d. Six silver atoms are present at the interface as shown on Figure 2.

Each two atoms are equivalent and hence have the same contribution which varies depending on the atom position with respect to the interface. The first and third atoms have the same contribution in the three configurations where there is a hybridization between Ag-4d (atom 1), As-4p and Fe-3d at -3.2 eV, while the fifth atom is characterized by the existence of four peaks where the highest appears at -4.62.

## CONCLUSION

The density functional theory (DFT) as implemented in the Quantum ESPRESSO PWSCF code was used for the study of the $Ag/BaFe_2As_2$ (001) interface. First, we calculated some electronic properties of the superconducting interface using the Generalized Gradient Approximation (GGA).The results obtained by calculating the distance between silver and superconducting $BaFe_2As_2$ showed that the most favorable sites for the deposition of silver atoms are intermediate sites. We found that the PDOS of Fe-3d and As-4p become close to each other indicating a strong hybridization of Fe-3d and As-4p states at the Fermi level region. This behavior is somehow similar to the density of state variation for $BaFe_2As_2$. The analysis of charge density reveals valuable information about bonding between atoms. States originating from Ag-4d orbitals, which become discernible at the lower part of the spectrum, are characterized by hybridization with Fe-4d and As-4p. Calculations of the electronic structure of the interface showed that the charge density increased slightly near the plane containing iron.

**REFERENCES**

[1]. Baker, F.C., Lampio, L., Saaresranta, T., et al., Sleep and sleep disorders in the menopausal transition. Sleep Med Clin, **2018**. 13(3):443-56.

[2]. Asltoghiri, M., Ghodsi, Z., The effects of Reflexology on sleep disorder in menopausal women. Procedia Soc Behav Sci, **2012**. 31:242-246.

[3]. Taavoni, S., Nazem, E., The Effect of lemon Balm on sleep disorder in menopausal women 60-50 years old. J Compl Med, **2013**. 2(4):344-54.

[4]. Taavoni, S., Ekbatani, N., Kashaniyan, M., et al., Menopause: effect of valerian on sleep quality in postmenopausal women: A randomized placebo-controlled clinical trial. Randomized Controlled Trial, **2011**. 16(3):286-287.

[5]. Bixler, E.O., Papaliaga, M.N., Vgontzas, A.N., Women sleep objectively better than men and the sleep of young women is more resilient to external stressors: effects of age and menopause. J Sleep Res, **2009**. 18(2):221-228.

[6]. Fund, N., Green, A., Chodick, G., et al. The epidemiology of sleep disorders in Israel: results from a population-wide study. Sleep Medicine, **2020**. 67:120-127.

[7]. Tao M, Sun D, Shao H, Li C, Teng YJBJoM, Research B. Poor sleep in middle-aged women is not associated with menopause per se. Braz J Med Biol Res, **2016**. 49(1):e4718.

[8]. Han, K.S, Kim, L., Shim, I., Stress and sleep disorder. Exp Neurobiol, **2012**. 21(4):141-50.

[9]. Venter, R., Role of sleep in performance and recovery of athletes: a review article. Phy Edu Rec, **2012**. 34(1):167-184.

[10]. Crowley, K., Sleep and sleep disorders in older adults. Neuropsychol Rev, **2011**. 21(1):41-53.

[11]. Polo, K.P., Sleep problems in midlife and beyond. Maturitas, **2011**. 68(3):224-232.

[12]. Xu, Q., Lang, C.P., Examining the relationship between subjective sleep disturbance and menopause: a systematic review and meta-analysis. Menopause, **2014**. 21(12):1301-1318.

[13]. Ornat, L., Martínez, D.R., Chedraui, P., Assessment of subjective sleep disturbance and related factors during female mid- life with the Jenkins Sleep Scale. Matutiras, **2014**. 77(4):344-350.

[14]. Sarris, J., Byrne, G.J,. A systematic review of insomnia and complementary medicine. Sleep Med Rev, **2011**. 15(2):99-106.

[15]. Cases, J., Ibarra, A., Feuillere, N., et al. Pilot trial of Melissa officinalis L. leaf extract in the treatment of volunteers suffering from mild-to-moderate anxiety disorders and sleep disturbances. Med J Nutrition Metab, **2011.** 4(3):211-218.

[16]. Lange, T., Dimitrov, S., Born, J. Effects of sleep and circadian rhythm on the human immune system. Ann N Y Acad Sci, **2010**. 1193(1):48-59.

[17]. Gooneratne, N.S., Complementary and alternative medicine for sleep disturbances in older adults. Clin Geriatr Med, **2008**. 24(1):121-38.

[18]. Haybar, H., Javid, A.Z., Haghighizadeh, M.H., et al. The effects of Melissa officinalis supplementation on depression, anxiety, stress, and sleep disorder in patients with chronic stable angina. Clin Nutr ESPEN, **2018**. 26:47-52.

[19]. Farrahi, J., Nakhaee, N., Sheibani, V., et al. Psychometric properties of the Persian version of the Pittsburgh Sleep Quality Index addendum for PTSD (PSQI-A). Sleep and Breathing, **2009**. 13(3):259-262.

[20]. Mohammadbeigi, A., Valizadeh, F., Saadati, M., et al. Sleep quality in medical students; the impact of over-use of mobile cell-phone and social networks. J Res Health Sci, **2016**. 16(1):46-50.

[21]. Moghaddam, J.F, Nakhaee, N., Sheibani, V., Reliability and validity of the Persian version of the Pittsburgh Sleep Quality Index (PSQI-P). Sleep Breath, **2012**. 16(1):79-82.
.
[22] Taavoni, S., Ekbatani, N., Haghani, H., Effect of Valerian and Lemon Balm Combined Capsules, On Postmenopausal Sleep Disorder, A Triple Blind Randomized Placebo Control Clinical Trial. Sleep Disorders and Stress, **2015**. 30:1784.